Effects of Sr addition on crystallinity and optical absorption edges in ternary semiconducting silicide $Ba_{1-x}Sr_xSi_2$

Kousuke Morita [a], Michitaka Kobayashi [a], Takashi Suemasu [a,b,*]

[a] *Institute of Applied Physics, University of Tsukuba, 1-1-1 Tennohdai, Tsukuba, Ibaraki 305-8573, Japan*
[b] *PRESTO, JST, 4-1-8 Honcho Kawaguchi, Saitama 332-0012, Japan*

Abstract

Polycrystalline $Ba_{1-x}Sr_xSi_2$ films with the Sr composition x varying from 0 to 0.77 were grown on transparent fused silica substrates by molecular beam epitaxy, and the effects of Sr addition on the indirect optical absorption edge E_{edge} were investigated. It was found that the E_{edge} value increases almost linearly with increasing x and reached approximately 1.40 eV when x was 0.52. When $x > 0.6$, the E_{edge} value almost saturates, and the formation of homogeneous $Ba_{1-x}Sr_xSi_2$ films became difficult. Composition separation was observed for $x = 0.77$.
© 2007 Elsevier B.V. All rights reserved.

Keywords: BaSi$_2$; Optical absorption; Solar cell; Molecular beam epitaxy

1. Introduction

Most solar cells currently produced are Si based. However, the band gap, E_g, of Si is as small as 1.1 eV at room temperature (RT). This value is approximately 0.3 eV smaller than the ideal band gap (~ 1.4 eV) that matches the solar spectrum [1]. This small E_g value for Si results in low photoelectric conversion efficiency of Si solar cells. In addition, approximately 200-μm-thick Si is required to form crystalline Si solar cells due to its small optical absorption coefficient α. Thus, new Si-based materials for high-efficiency thin-film solar cells are needed. Semiconducting orthorhombic barium disilicide (BaSi$_2$) is thought to be a good candidate for such a material.

The E_g value of BaSi$_2$ has been previously ascertained from the temperature dependence of resistivity and diffuse reflectance spectra in bulk BaSi$_2$ [2,3] and from scanning tunneling spectroscopy results of a few-monolayer-thick BaSi$_2$ films on Si [4], to be approximately 1.1–1.3 eV at RT. The optical absorption spectra of polycrystalline BaSi$_2$ films on transparent fused silica substrates show that its indirect absorption edge E_{edge} is approximately 1.3 eV. In addition, α reaches 10^5 cm^{-1} at 1.5 eV [5], which is approximately two orders of magnitude higher than the value for Si. This large α is thought to come from the contribution of the Ba $5d$ state to both the conduction and valence bands in BaSi$_2$ [6]. From the viewpoint of application to solar cells, it is desirable to increase the band gap to 1.4 eV by applying band-gap engineering to BaSi$_2$, that is, by replacing some of the Ba atoms with isoelectric alkaline-earth metal atoms. The formation of $Ba_{1-x}Sr_xSi_2$ bulk itself has already been reported [7]. However, there were no descriptions of its optical properties. We have realized epitaxial growth of BaSi$_2$ and $Ba_{1-x}Sr_xSi_2$ on Si(111) by molecular beam epitaxy (MBE) [8–11]. X-ray diffraction (XRD) measurements revealed that the a-axis lattice constant of $Ba_{1-x}Sr_xSi_2$ decreases linearly with increasing Sr composition x [10]. Very recently, we reported that the indirect optical absorption edge E_{edge} in $Ba_{1-x}Sr_xSi_2$ increases almost linearly with increasing Sr composition x when $0 \le x \le 0.5$ [12].

The purpose of this study is to investigate the details of the effect of Sr addition on crystallinity and optical absorption properties of $Ba_{1-x}Sr_xSi_2$. For this purpose, we prepared $Ba_{1-x}Sr_xSi_2$ films with different x values on transparent fused silica substrates covered with pre-deposited polycrystalline Si layers. The composition separation and saturation of E_{edge} in $Ba_{1-x}Sr_xSi_2$ with Sr compositions higher than 0.6 are described.

2. Experimental

An ion-pumped MBE system equipped with standard Knudsen cells for Ba and Sr, and an electron-beam evaporation source for Si was used. Transparent fused silica substrates

---

covered with 100-nm-thick polycrystalline Si layers were used, so that the contribution of the substrate to the measured optical absorption spectra would be small [5]. The pre-deposited Si layers prevent diffusion of O atoms from the substrate into the grown layers. After hydrogen termination of the Si surfaces that were etched by a HF solution, the wafers were thermally cleaned in UHV. Polycrystalline $Ba_{1-x}Sr_xSi_2$ films with various x values ranging from 0 to 0.77 were then grown using MBE. The thickness of the grown layers was approximately 200 nm. Details of the growth procedure have been described in our previous papers [5,12]. The crystalline quality of $Ba_{1-x}Sr_xSi_2$ was characterized by XRD measurements. The composition of the grown layers was evaluated by Rutherford backscattering spectroscopy (RBS) measurements using $^4He^+$ ions accelerated at 2.3 MeV. The optical absorption spectra of $Ba_{1-x}Sr_xSi_2$ were measured at RT using a double-beam spectrophotometer (JASCO V570) in a transmission configuration.

3. Results and discussion

RBS and XRD measurements were performed in order to confirm the formation of $Ba_{1-x}Sr_xSi_2$ films. The RBS random spectra obtained experimentally were reproduced by simulations, and the Sr composition was then derived. Fig. 1(a) and (b) show the RBS depth profiles of Ba, Sr, Si and O atoms in $Ba_{1-x}Sr_xSi_2$ for $x=0.29$ and 0.52. Ba and Sr were homogeneously distributed, and the Ba plus Sr ratio to Si was 0.5 in the grown layers. Similar results were obtained for $Ba_{1-x}Sr_xSi_2$ when x was lower than 0.6. On the other hand, several samples were prepared wherein x was higher than 0.6; however, we have not yet succeeded in forming $Ba_{1-x}Sr_xSi_2$ with homogeneous Ba and Sr distributions, as shown in Fig. 1(c) and (d). Values of x of 0.64 and 0.77 were obtained, assuming that the Sr atoms were homogeneously distributed in the grown layers.

The θ-2θ XRD patterns of polycrystalline $Ba_{1-x}Sr_xSi_2$ for $x=0$, 0.29, 0.52, 0.64 and 0.77 are shown in Fig. 2(a)–(e),

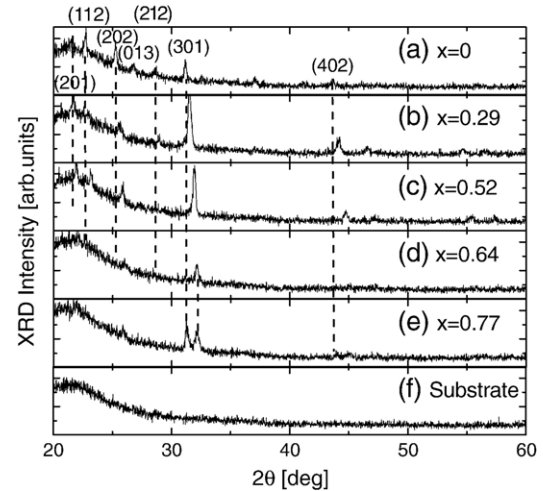Fig. 2. θ-2θ XRD patterns of $Ba_{1-x}Sr_xSi_2$ films grown on transparent fused silica substrates when x is (a) 0, (b) 0.29, (c) 0.52, (d) 0.64, and (e) 0.77; (f) is the XRD pattern of the substrate used. The dotted lines are guides to the eye.

respectively. The origin of the broad diffraction peak seen at ~21° in all the samples is the substrate, as seen from Fig. 2(f). All the diffraction peaks seen in the sample without Sr addition (Fig. 2(a)) correspond to $BaSi_2$, and they shifted clearly to a high-angle-region with increasing x as shown in Fig. 2(a)–(d). The dotted lines are guides to the eye. This result indicates that the lattice spacing of the film decreased with increasing x. The atomic radius of Sr is smaller than that of Ba. Thus, when some Ba atoms in the $BaSi_2$ lattice structure are replaced by Sr atoms, this kind of lattice contraction will take place. It was found from XRD peak positions that a, b and c lattice constants in $Ba_{1-x}Sr_xSi_2$ decreased linearly with increasing x. Detailed results will be reported elsewhere. Similar lattice contraction is observed in $Ca_{1-x}Ba_xF_2$ [13], which is completely miscible and obeys Vegards law across the entire composition range. In contrast, the diffraction peak of the (301) plane splits into two peaks in the sample with $x=0.77$ as shown in Fig. 2(e). The
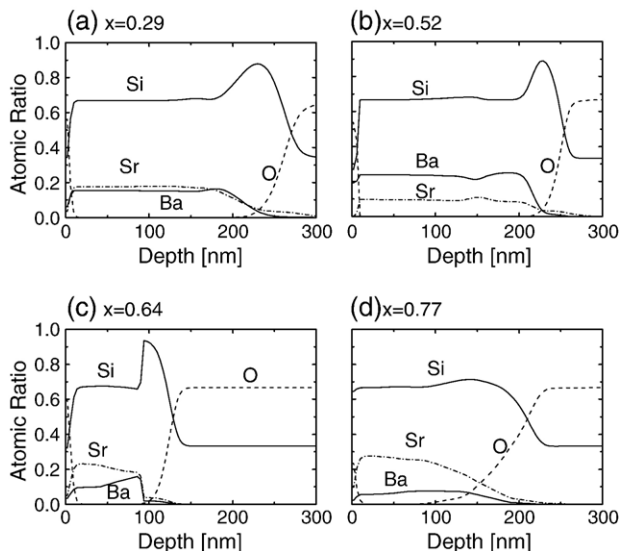

Fig. 1. RBS depth profiles of Si, Ba, Sr and O atoms for $Ba_{1-x}Sr_xSi_2$ grown on transparent fused silica substrates when x is (a) 0.29, (b) 0.52, (c) 0.64 and (d) 0.77.
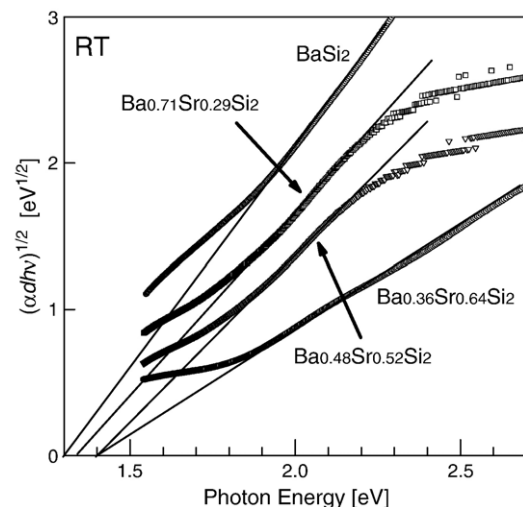

Fig. 3. $(\alpha dh\nu)^{1/2}$ vs. $h\nu$ plots for 100-nm-thick $BaSi_2$, 200-nm-thick $Ba_{0.71}Sr_{0.29}Si_2$ and $Ba_{0.48}Sr_{0.52}Si_2$, and 100-nm-thick $Ba_{0.36}Sr_{0.64}Si_2$ measured at RT.
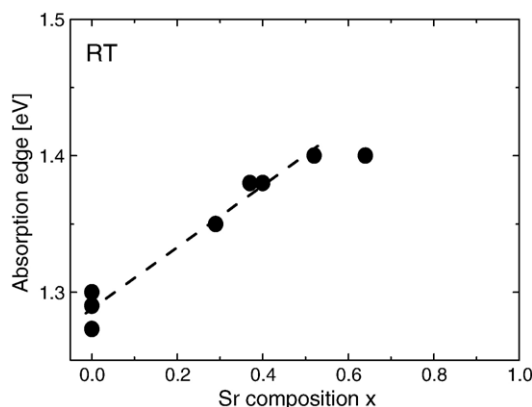
Fig. 4. Sr composition, x, dependence of indirect absorption edges in $Ba_{1-x}Sr_xSi_2$ measured at RT.

peak position of the low-angle diffraction is the same as that of the $BaSi_2$(301) plane. Thus, the high-angle diffraction is thought to correspond to the (301) plane of $Ba_{1-x}Sr_xSi_2$. The peak position of the (301) plane of $Ba_{1-x}Sr_xSi_2$ does not change between $x=0.64$ and 0.77. Therefore, the additional Sr might segregate in the form of Sr-Si silicides. $Ba_{1-x}Sr_xSi_2$ is not stable for high Sr content because $SrSi_2$ with a $BaSi_2$-type structure does not exist at RT. Composition separation is therefore thought to take place for high Sr content.

Fig. 3 shows $(\alpha dh\nu)^{1/2}$ vs. $h\nu$ plots obtained for the 100-nm-thick $BaSi_2$, 200-nm-thick $Ba_{0.71}Sr_{0.29}Si_2$ and $Ba_{0.48}Sr_{0.52}Si_2$, and 100-nm-thick $Ba_{0.36}Sr_{0.64}Si_2$ at RT, where $h\nu$ is the photon energy, and d the thickness of the grown layers. The $(\alpha dh\nu)^{1/2}$ values of $Ba_{1-x}Sr_xSi_2$ ($x=0.29$, 0.52 and 0.64) are multiplied by some factors, so that the plots shift downwards or upwards to be distinguished in Fig. 3. This operation does not affect the optical absorption edges. The influence of the pre-deposited polycrystalline Si layer and the fused silica substrate was already subtracted by comparing the transmittance measured on the samples with and without the grown layers. The plots are fitted to straight lines, showing that $BaSi_2$ and $Ba_{1-x}Sr_xSi_2$ are indirect band gap semiconductors. The indirect absorption edge, E_{edge}, with phonon emission is thus obtained from the intersection of the straight line with the horizontal axis. The values of E_{edge} obtained for $BaSi_2$ and $Ba_{1-x}Sr_xSi_2$ ($x=0.29$, 0.52 and 0.64) were 1.30, 1.35, 1.40 and 1.40 eV, respectively, as shown in Fig. 3. Indirect absorption by phonon absorption is neglected, because the fitting was performed at a higher energy region than the indirect band gap. An alternative interpretation of this absorption edge is the presence of the Urbach tail. However, a plot of α vs. $h\nu$ did not yield an exponential dependence. Therefore, the absorption edge can be better interpreted as being due to indirect absorption rather than due to the Urbach tail absorption.

The E_{edge} values of the other samples were derived in the same way, and are summarized in Fig. 4 which shows E_{edge} as a function of x in $Ba_{1-x}Sr_xSi_2$ measured at RT. It was found that E_{edge} increases almost linearly with increasing x and reaches approximately 1.40 eV when x is 0.52. This suggests that the

band gap of $BaSi_2$ is increased by the addition of Sr. It was also found that E_{edge} slightly scatters, depending on its thickness (see the E_{edge} of $BaSi_2$); however, the dispersion of E_{edge} was 30 meV at most. On the basis of the above results, we conclude that E_{edge} of $Ba_{1-x}Sr_xSi_2$ is increased by approximately 0.1 eV by increasing the Sr composition x up to 0.52. On the other hand, the E_{edge} value almost saturates for $Ba_{1-x}Sr_xSi_2$ when x is 0.64. Taking into account the fact that the formation of $Ba_{1-x}Sr_xSi_2$ with $x>0.6$ is difficult, as described above, it can be stated that the expansion of E_{edge} in $Ba_{1-x}Sr_xSi_2$ is limited up to approximately 1.4 eV.

4. Conclusions

$Ba_{1-x}Sr_xSi_2$ films with various Sr compositions were grown on transparent fused silica substrates by MBE, and the effects of Sr addition on the crystallinity and optical absorption properties were investigated. $Ba_{1-x}Sr_xSi_2$ films with homogeneous Ba and Sr distributions were obtained when $x<0.5$. The E_{edge} value increased almost linearly with increasing x and reached approximately 1.40 eV when x was 0.52. On the other hand, for higher x values, the E_{edge} value saturated, and the formation of homogeneous $Ba_{1-x}Sr_xSi_2$ films itself was difficult for samples in which $x>0.6$ since composition separation occurred.

Acknowledgements

References

[1] S.M. Sze, Physics of Semiconductor Devices, 2nd ed.Wiley, New York, 1981.
[2] J. Evers, A. Weiss, Mater. Res. Bull. 9 (1974) 549.
[3] T. Nakamura, T. Suemasu, K. Takakura, F. Hasegawa, A. Wakahara, M. Imai, Appl. Phys. Lett. 81 (2002) 1032.
[4] K. Ojima, M. Yoshimura, K. Ueda, Jpn. J. Appl. Phys., Part 1 41 (2002) 4965.
[5] K. Morita, Y. Inomata, T. Suemasu, Thin Solid Films 508 (2006) 363.
[6] Y. Imai, A. Watanabe, M. Mukaida, J. Alloys Compd. 358 (2003) 257.
[7] J. Evers, J. Solid State Chem. 32 (1980) 77.
[8] Y. Inomata, T. Nakamura, T. Suemasu, Jpn. J. Appl. Phys., Part 1 43 (2004) 4155.
[9] Y. Inomata, T. Nakamura, T. Suemasu, F. Hasegawa, Jpn. J. Appl. Phys., Part 2 43 (2004) L478.
[10] Y. Inomata, T. Suemasu, T. Izawa, F. Hasegawa, Jpn. J. Appl. Phys., Part 2 43 (2004) L771.
[11] T. Suemasu, K. Morita, M. Kobayashi, M. Saida, M. Sasaki, Jpn. J. Appl. Phys., Part 2 45 (2006) L519.
[12] K. Morita, M. Kobayashi, T. Suemasu, Jpn. J. Appl. Phys., Part 2 45 (2006) L390.
[13] H. Zogg, M. Hüppi, Appl. Phys. Lett. 47 (1985) 133.